



LAWRENCE
LIVERMORE
NATIONAL
LABORATORY

Nuclear Energy Density Optimization: UNEDF2

M. Kortelainen, J. McDonnell, W. Nazarewicz, E. Olsen,
P. G. Reinhard, J. Sarich, N. Schunck, S. M. Wild, D.
Davesne, J. Erler, A. Pastore

November 5, 2014

2nd Conference on "Advances in Radioactive Isotope Science"
(ARIS2014)

Tokyo, Japan

June 1, 2014 through June 6, 2014

Disclaimer

This document was prepared as an account of work sponsored by an agency of the United States government. Neither the United States government nor Lawrence Livermore National Security, LLC, nor any of their employees makes any warranty, expressed or implied, or assumes any legal liability or responsibility for the accuracy, completeness, or usefulness of any information, apparatus, product, or process disclosed, or represents that its use would not infringe privately owned rights. Reference herein to any specific commercial product, process, or service by trade name, trademark, manufacturer, or otherwise does not necessarily constitute or imply its endorsement, recommendation, or favoring by the United States government or Lawrence Livermore National Security, LLC. The views and opinions of authors expressed herein do not necessarily state or reflect those of the United States government or Lawrence Livermore National Security, LLC, and shall not be used for advertising or product endorsement purposes.

Nuclear Energy Density Optimization: UNEDF2

M. Kortelainen^{1,2,3,4}, J. McDonnell^{3,4,5}, W. Nazarewicz^{3,4,6}, E. Olsen³, P.-G. Reinhard⁷, J. Sarich⁸, N. Schunck^{5,3,4}, S. M. Wild⁸, D. Davesne⁹, J. Erler¹⁰, A. Pastore¹¹

¹*Department of Physics, University of Jyväskylä, P.O. Box 35 (YFL), FI-40014 Jyväskylä, Finland*

²*Helsinki Institute of Physics, P.O. Box 64, FI-00014 University of Helsinki, Finland*

³*Department of Physics and Astronomy, University of Tennessee, Knoxville, TN 37996, USA*

⁴*Physics Division, Oak Ridge National Laboratory, Oak Ridge, TN 37831, USA*

⁵*Physics Division, Lawrence Livermore National Laboratory, Livermore, CA 94551, USA*

⁶*Institute of Theoretical Physics, Warsaw University, ul. Hoża 69, PL-00681, Warsaw, Poland*

⁷*Institut für Theoretische Physik, Universität Erlangen, D-91054 Erlangen, Germany*

⁸*Mathematics and Computer Science Division, Argonne National Laboratory, Argonne, IL 60439, USA*

⁹*Institut de Physique Nucléaire de Lyon, CNRS-IN2P3, UMR 5822, Université Lyon 1, F-69622 Villeurbanne, France*

¹⁰*Division of Biophysics of Macromolecules, German Cancer Research Center (DKFZ), Im Neuenheimer Feld 580, D-69120 Heidelberg, Germany*

¹¹*Institut d'Astronomie et d'Astrophysique, Université Libre de Bruxelles - CP226, 1050 Brussels, Belgium*

E-mail: markus.kortelainen@jyu.fi

The parameters of the UNEDF2 nuclear energy density functional (EDF) model were obtained in an optimization to experimental data consisting of nuclear binding energies, proton radii, odd-even mass staggering data, fission-isomer excitation energies, and single particle energies. In addition to parameter optimization, sensitivity analysis was done to obtain parameter uncertainties and correlations. The resulting UNEDF2 is an all-around EDF. However, the sensitivity analysis also demonstrated that the limits of current Skyrme-like EDFs have been reached and that novel approaches are called for.

KEYWORDS: nuclear density functional theory, Skyrme energy density

1. Introduction

The development of a universal nuclear energy density functional (EDF) capable of explaining and predicting static and dynamic properties of atomic nuclei is one of the important goals in the low-energy nuclear physics. This was also one of the main research efforts in the UNEDF SciDAC-2 project [1]. During this project, the Skyrme-like EDFs UNEDF0 [2], UNEDF1 [3], and UNEDF2 [4] were developed. The nuclear EDF is a key element in the nuclear density functional theory (DFT). At present, DFT is the only microscopic theory which can be applied throughout the entire nuclear landscape. Because parameters of the nuclear EDF cannot be precalculated with sufficient accuracy from any theory, they must be calibrated to experimental input. An important aspect of the UNEDF project and the calibration of these EDFs was the joint collaboration of physicists, applied mathematicians, and computer scientists working together toward a common goal.

With the UNEDF0 EDF we established our EDF parameter optimization procedure. By incorporating recent developments in optimization techniques and increased computational power, the optimization could be carried out for the first time at the deformed Hartree-Fock-Bogoliubov (HFB) level. Since deformation properties of UNEDF0 were found to be inadequate, the UNEDF1 optimization paid attention to the fission properties in the actinide region. With the inclusion of data points on

fission isomer excitation energies, the resulting UNEDF1 EDF reproduced fission barriers in actinides well. The optimization of UNEDF2 focused on the shell structure. Here, the tensor part of the EDF was also included in the set of optimized parameters. To constrain tensor coupling constants, data from single-particle levels was included in the experimental data set. In addition to parameter optimization, all UNEDF parameterizations also provided results from the sensitivity analysis.

2. Theoretical framework

In the Skyrme-EDF framework, the total energy of a nucleus is a functional of the one-body density matrix ρ and the pairing density matrix $\tilde{\rho}$. The total energy is a sum of kinetic energy, Skyrme energy, pairing energy, and Coulomb energy. The time-even part of the Skyrme energy density reads

$$\mathcal{E}_t^{\text{Sk}}(\mathbf{r}) = C_t^\rho[\rho_0(\mathbf{r})]\rho_t^2(\mathbf{r}) + C_t^\tau\rho_t(\mathbf{r})\tau_t(\mathbf{r}) + C_t^{\Delta\rho}\rho_t(\mathbf{r})\Delta\rho_t(\mathbf{r}) + C_t^{\nabla J}(\mathbf{r})\rho_t(\mathbf{r})\nabla \cdot \mathbf{J}_t(\mathbf{r}) + C_t^J\mathbb{J}_t^2(\mathbf{r}), \quad (1)$$

which is composed of isoscalar ($t = 0$) and isovector ($t = 1$) densities. The density dependent coupling constant in Eq. (1) is defined by

$$C_t^\rho[\rho_0(\mathbf{r})] = C_{t0}^\rho + C_{tD}^\rho\rho_0^\gamma(\mathbf{r}). \quad (2)$$

Standard definitions of densities appearing in Eq. (1) can be found in Ref. [5]. The volume coupling constants, $\{C_{t0}^\rho, C_{tD}^\rho, C_t^\tau, \gamma\}$, can be related to the infinite nuclear matter (INM) parameters [2]. In all UNEDF energy density optimizations the volume part was expressed by these INM parameters. In addition to the Skyrme energy density part, the pairing term was taken to be the mixed type pairing force of Ref. [6], with V_0^n and V_0^p as the corresponding neutron and proton pairing strengths, respectively.

The optimization of UNEDF2 was done by minimizing an objective function $\chi^2(\mathbf{x})$ with respect to the model parameters \mathbf{x} ,

$$\chi^2(\mathbf{x}) = \frac{1}{n_d - n_x} \sum_{i=1}^{n_d} \left(\frac{s_i(\mathbf{x}) - d_i}{w_i} \right)^2, \quad (3)$$

where n_d and n_x are the number of data points and number of model parameters, respectively. Furthermore, $s_i(\mathbf{x})$ is the value of the i th observable, as predicted by the model and d_i is the corresponding experimental value. The experimental data set consisted of binding energies of 29 spherical and 47 deformed nuclei, 13 odd-even mass staggering (OEM) data points, 28 proton radii, 4 fission isomer excitation energies, and 9 single-particle (sp) level energy splittings. The used experimental proton radii values were deduced from the measured charge radii. Lastly, w_i in Eq. (3) is the weight of the i th observable. Here, the selected weights were 2 MeV for binding energies, 0.02 fm for proton radii, 0.1 MeV for OEM data, 0.5 MeV for fission isomer excitation energies, and 1.2 MeV for sp-level energies.

3. The UNEDF2 energy density

The optimization of all UNEDF EDFs was carried out at the axially deformed HFB level, with the computer code HFBTHO [7]. This code solves the HFB equations in an axially symmetric deformed harmonic oscillator (HO) basis. All the nuclei were computed in a space of 20 major HO shells. Similarly to the UNEDF0 and UNEDF1 parameterizations, the optimization was carried out by using the POUNDERS algorithm [8], which was found to be significantly faster compared to the traditionally used Nelder-Mead algorithm [2]. The UNEDF2 optimization utilized a hybrid parallel OpenMP+MPI scheme. Similarly to the UNEDF0 and UNEDF1 optimizations, the parameters of the functional were not allowed to attain unphysical values, so bounds were imposed on the range of variation for each parameter.

In addition to the optimization, we did a complete sensitivity analysis for the optimized parameter set in order to obtain standard deviations and correlations of the model parameters. The sensitivity analysis provides useful information about which of the parameters are strongly correlated and which of the parameters are poorly determined by the employed data set. This analysis also can be used to estimate the impact of one data point on the position of the $\chi^2(\mathbf{x})$ minimum. Most importantly, sensitivity analysis is an important tool when addressing the predictive power of the model and associated model uncertainties. Once the covariance matrix is known, the model errors can be propagated [9–14]. In particular, when an EDF model is used in extrapolation to an experimentally unknown region, the role of the model errors becomes prominent.

A numerical criterion, based on linear response theory in symmetric nuclear matter, was established in Ref. [15] to determine the eventual presence of finite-size instabilities in calculations of the nuclei. We verified that UNEDF2 respects this criterion, thus making it a reliable EDF for the calculation of finite nuclei.

Table I. The UNEDF2 parameterization. Listed are parameter name, parameter value, and standard deviation σ for each parameter. Energy per particle (E), nuclear matter incompressibility (K), symmetry energy (a_{sym}), and the slope of symmetry energy (L) are in units of MeV, saturation density (ρ_c) is in units of fm^{-3} , scalar effective mass ($1/M_s^*$) is unitless, $C_t^{\Delta\rho}$, $C_t^{\nabla J}$, and C_t^J are in units of MeV fm^5 , and $V_0^{n/p}$ is in units of MeV fm^3 .

Parameter	Value	σ	Parameter	Value	σ
E	-15.8	N/a	$C_0^{\Delta\rho}$	-46.831	2.689
ρ_c	0.15631	0.00112	$C_1^{\Delta\rho}$	-113.164	24.322
K	239.930	10.119	V_0^n	-208.889	8.353
$1/M_s^*$	1.074	0.052	V_0^p	-230.330	6.792
a_{sym}	29.131	0.321	$C_0^{\nabla J}$	-64.309	5.841
L	40.0	N/a	$C_1^{\nabla J}$	-38.650	15.479
			C_0^J	-54.433	16.481
			C_1^J	-65.903	17.798

Table I lists the UNEDF2 parameterization, along with the corresponding parameter standard deviations. The volume part of the EDF, expressed by INM parameters, is listed in the left column. In the sensitivity analysis, the parameters that hit the set boundaries during the optimization were excluded. Also, since the data set was incapable of constraining the vector effective mass, the SLy4 value of $1/M_v^* \approx 1.250$ was used [16]. (See the supplementary material of Ref. [4] for precise presentation of the parameterization.) When comparing UNEDF2 parameter uncertainties to those of UNEDF1, the UNEDF2 parameters usually have the same or smaller magnitude. Furthermore, the parameter uncertainty interval with UNEDF1 is usually narrower compared to UNEDF0, which indicates that the UNEDF2 EDF is better constrained with the current data, and – given the current observables – any major further improvement is unlikely.

The nuclear ground-state properties predicted by the UNEDF2 EDF were computed for the whole even-even nuclear landscape. This was done with a parallel calculation scheme where each nucleus was distributed to a separate CPU core [18]. The same setup was also used for evaluation of the systematic error for the boundaries of the nuclear landscape, as predicted by various Skyrme-EDF models [19]. Fig. 1 shows the calculated residuals of the even-even nuclear binding energies with the UNEDF2 EDF. As shown, the residuals are not randomly distributed, and clear arc-like features can be seen, common to many mean-field methods. This is one indication that Skyrme-like models are lacking some physics. The total root-mean-square (r.m.s.) deviation from the experimental data was 1.95 MeV, which is a bit higher compared to 1.43 MeV for UNEDF0, but similar to the 1.91 MeV for

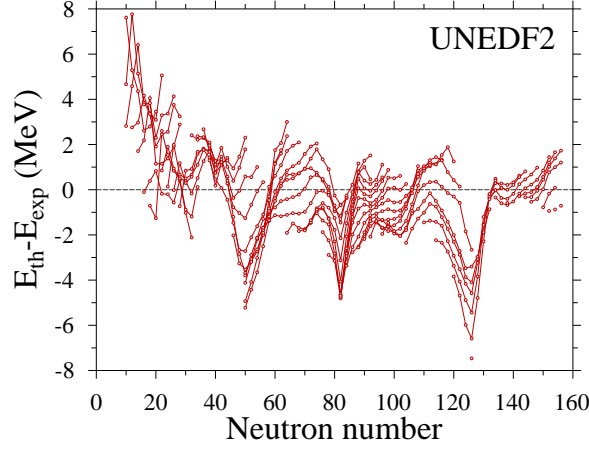


Fig. 1. The residuals of the even-even nuclear binding energies, calculated with UNEDF2, compared to experimental data of Ref. [17]. The lines indicate isotopic chains.

UNEDF1. For two-neutron separation energies, the r.m.s. deviation of UNEDF2 was 0.84 MeV and for two-proton separation energies the r.m.s. deviation was 0.78 MeV. With these observables, the r.m.s. deviation for UNEDF0 and UNEDF1 was similar in magnitude. With the proton radii, the UNEDF2 r.m.s. deviation was 0.018 fm, which is about the same as UNEDF0 and UNEDF1.

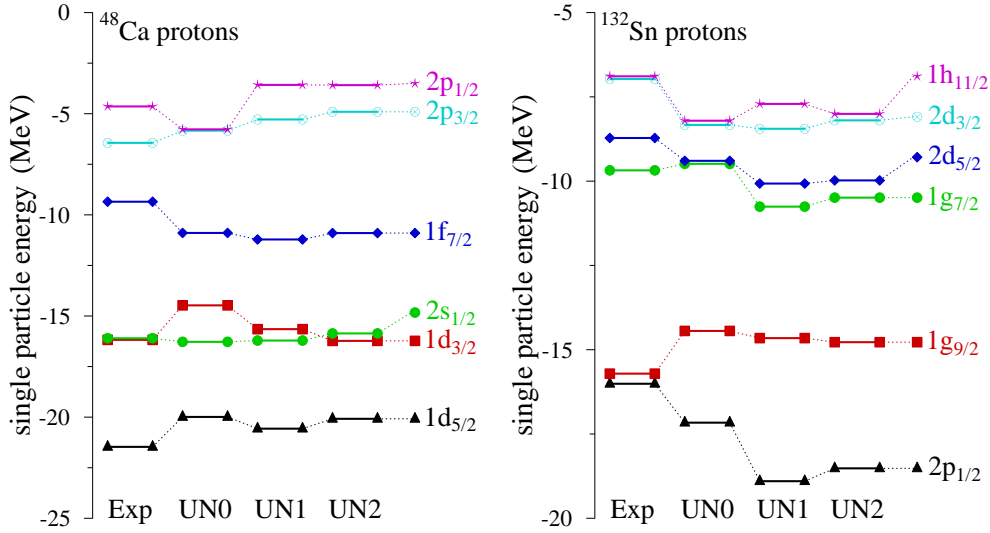


Fig. 2. Calculated proton single particle energies in ^{48}Ca and ^{132}Sn with UNEDF0 (UN0), UNEDF1 (UN1), and UNEDF2 (UN2) EDFs compared to the experimental data of Ref. [20]. The experimental data were deduced from the spectra of neighboring odd-even nucleus and the binding energy differences between doubly magic nuclei and their corresponding odd-even neighbors.

As mentioned, one focal point of the UNEDF2 study was the shell structure. Fig. 2 shows proton single particle (sp) levels in ^{48}Ca and ^{132}Sn as calculated with UNEDF EDFs. All the sp-levels here, as well as during the optimization of UNEDF2, were calculated within the equal filling quasiparticle blocking procedure. The total r.m.s. deviation of the sp-levels in doubly-magic nuclei with UNEDF2,

from the experimental levels of Ref. [20], was 1.38 MeV. This is close to the best possible r.m.s. deviation that can be attained with a Skyrme-like EDF [21]. The two-particle separation energies across the shell gaps of doubly-magic nuclei were reproduced better with UNEDF2 when compared to UNEDF0 and UNEDF1.

4. Conclusions

The UNEDF2 EDF was optimized to the experimental data set containing a rather large variety of observable types. The optimization also included tensor coupling constants, which could be constrained due to the expanded data set used. The performance of UNEDF2 was tested against various experimental data [4]. Global properties were found to be on par with the previous UNEDF1 parameterization. Fission properties of UNEDF2 were slightly degraded from those of UNEDF1, particularly for the outer barrier heights. The UNEDF2 EDF can be viewed as a balanced all-around EDF.

In addition to parameter optimization, sensitivity analysis was done to obtain parameter uncertainties and correlations. This sensitivity analysis clearly demonstrated that the limits of current Skyrme-like EDFs have been reached and that novel approaches are called for. Similar conclusions were obtained in other studies, that is, any further major improvements with Skyrme-like EDFs are unlikely [21, 22]. To improve the current situation, new theoretical efforts have been launched. For example, the novel EDFs with higher order terms [23–26] or enriched density dependence [27, 28] could capture more physics and reduce systematic errors in theory.

Acknowledgments

This work was supported by the U.S. Department of Energy under Contract Nos. DE-SC0008499, DE-FG02-96ER40963, and DE-FG52-09NA29461 (University of Tennessee), DE-AC02-06CH11357 (Argonne National Laboratory), and DE-AC52-07NA27344 (Lawrence Livermore National Laboratory); by the Academy of Finland under the Centre of Excellence Programme 2012-2017 (Nuclear and Accelerator Based Physics Programme at JYFL) and the FIDIPRO programme; and by the European Union’s Seventh Framework Programme ENSAR (THEXO) under Grant No. 262010.

Computational resources were provided through an INCITE award “Computational Nuclear Structure” by the National Center for Computational Sciences (NCCS) and National Institute for Computational Sciences (NICS) at Oak Ridge National Laboratory, through a grant by the Livermore Computing Resource Center at Lawrence Livermore National Laboratory, and through a grant by the Laboratory Computing Resource Center at Argonne National Laboratory.

References

- [1] S. Bogner, A. Bulgac, J. Carlson, J. Engel, G. Fann, R. Furnstahl, S. Gandolfi, G. Hagen, M. Horoi, C. Johnson, M. Kortelainen, E. Lusk, P. Maris, H. Nam, P. Navratil, W. Nazarewicz, E. Ng, G. Nobre, E. Ormand, T. Papenbrock, J. Pei, S. Pieper, S. Quaglioni, K. Roche, J. Sarich, N. Schunck, M. Sosonkina, J. Terasaki, I. Thompson, J. Vary, and S. Wild: *Comput. Phys. Comm.* **184** (2013) 2235.
- [2] M. Kortelainen, T. Lesinski, J. Moré, W. Nazarewicz, J. Sarich, N. Schunck, M. V. Stoitsov, and S. Wild: *Phys. Rev. C* **82** (2010) 024313.
- [3] M. Kortelainen, J. McDonnell, W. Nazarewicz, P.-G. Reinhard, J. Sarich, N. Schunck, M. V. Stoitsov, and S. M. Wild: *Phys. Rev. C* **85** (2012) 024304.
- [4] M. Kortelainen, J. McDonnell, W. Nazarewicz, E. Olsen, P.-G. Reinhard, J. Sarich, N. Schunck, S. M. Wild, D. Davesne, J. Erler, and A. Pastore: *Phys. Rev. C* **89** (2014) 054314.
- [5] M. Bender, P.-H. Heenen, and P.-G. Reinhard: *Rev. Mod. Phys.* **75** (2003) 121.
- [6] J. Dobaczewski, W. Nazarewicz, and M. V. Stoitsov: *Eur. Phys. J. A* **15** (2002) 21.
- [7] M. V. Stoitsov, N. Schunck, M. Kortelainen, N. Michel, H. Nam, E. Olsen, J. Sarich, and S. Wild: *Comput. Phys. Comm.* **184** (2013) 1592.

- [8] S. M. Wild, J. Sarich, and N. Schunck: arXiv:1406.5464 (2014).
- [9] Y. Gao, J. Dobaczewski, M. Kortelainen, J. Toivanen, and D. Tarpanov: Phys. Rev. C **87** (2013) 034324.
- [10] M. Kortelainen, J. Erler, W. Nazarewicz, N. Birge, Y. Gao, and E. Olsen: Phys. Rev. C **88** (2013) 031305.
- [11] J. Dobaczewski, W. Nazarewicz, and P.-G. Reinhard: J. Phys. G **41** (2014) 074001.
- [12] N. Schunck, J. D. McDonnell, J. Sarich, S. M. Wild, and D. Higdon: arXiv:1406.4383 (2014).
- [13] J. Erler and P.-G. Reinhard: arXiv:1408.0208 (2014).
- [14] M. Kortelainen: arXiv:1409.1413 (2014).
- [15] V. Hellemans, A. Pastore, T. Duguet, K. Bennaceur, D. Davesne, J. Meyer, M. Bender, and P.-H. Heenen: Phys. Rev. C **88** (2013) 064323.
- [16] E. Chabanat, P. Bonche, P. Haensel, J. Meyer, and R. Schaeffer: Nucl. Phys. A **635** (1998) 231.
- [17] G. Audi, A.H. Wapstra, and C. Thibault, Nucl. Phys. A **729**, 337 (2003).
- [18] J. Erler, N. Birge, M. Kortelainen, W. Nazarewicz, E. Olsen, A. Perhac, and M. Stoitsov: J. Phys. Conf. Ser. **402** (2012) 012030.
- [19] J. Erler, N. Birge, M. Kortelainen, W. Nazarewicz, E. Olsen, A. Perhac, and M. Stoitsov: Nature **486** (2012) 509.
- [20] N. Schwierz, I. Wiedenhover, and A. Volya: arXiv:0709.3525 (2007).
- [21] M. Kortelainen, J. Dobaczewski, K. Mizuyama, and J. Toivanen: Phys. Rev. C **77** (2008) 064307.
- [22] D. Tarpanov, J. Dobaczewski, J. Toivanen, and B.G. Carlsson, arXiv:1405.4823 (2014).
- [23] B. G. Carlsson, J. Dobaczewski, and M. Kortelainen: Phys. Rev. C **78** (2008) 044326.
- [24] J. Dobaczewski, K. Bennaceur, and F. Raimondi: J. Phys. G **39** (2012) 125103.
- [25] F. Raimondi, K. Bennaceur, and J. Dobaczewski: J. Phys. G **41** (2014) 055112.
- [26] P. Becker, D. Davesne, J. Meyer, A. Pastore, and J. Navarro: arXiv:1406.0340 (2014).
- [27] B. Gebremariam, T. Duguet, and S. K. Bogner: Phys. Rev. C **82** (2010) 014305.
- [28] M. Stoitsov, M. Kortelainen, S. K. Bogner, T. Duguet, R. J. Furnstahl, B. Gebremariam, and N. Schunck: Phys. Rev. C **82** (2010) 054307.